the plant journal

SEB Society for Experimental Biology

The Plant Journal (2018) **94,** 857–866 doi: 10.1111/tpj.13903

Analysis of the functions of *TaGW2* homoeologs in wheat grain weight and protein content traits

Yi Zhang[1,2,3,†], Da Li[1,2,†], Dingbo Zhang[1,2], Xiaoge Zhao[1,2], Xuemin Cao[1,2], Lingli Dong[1], Jinxing Liu[1], Kunling Chen[1], Huawei Zhang[1], Caixia Gao[1,*] and Daowen Wang[1,2,*]

[1]*The State Key Laboratory of Plant Cell and Chromosome Engineering, and Center for Genome Editing, Institute of Genetics and Developmental Biology, Chinese Academy of Sciences, Beijing 100101, China,*

[2]*University of Chinese Academy of Sciences, Beijing 100049, China, and*

[3]*Key Laboratory of Plant Stress Research, College of Life Science, Shandong Normal University, Jinan 250014, China*

Received 17 October 2017; revised 2 March 2018; accepted 6 March 2018; published online 23 March 2018.

*For correspondence (e-mails cxgao@genetics.ac.cn; dwwang@genetics.ac.cn).

†These authors contributed equally to this article.

SUMMARY

***GW2* is emerging as a key genetic determinant of grain weight in cereal crops; it has three homoeologs (*TaGW2-A1*, *-B1* and *-D1*) in hexaploid common wheat (*Triticum aestivum* L.). Here, by analyzing the gene editing mutants that lack one (*B1* or *D1*), two (*B1* and *D1*) or all three (*A1*, *B1* and *D1*) homoeologs of *TaGW2*, several insights are gained into the functions of *TaGW2-B1* and *-D1* in common wheat grain traits. First, both *TaGW2-B1* and *-D1* affect thousand-grain weight (TGW) by influencing grain width and length, but the effect conferred by *TaGW2-B1* is stronger than that of *TaGW2-D1*. Second, there exists functional interaction between *TaGW2* homoeologs because the TGW increase shown by a double mutant (lacking *B1* and *D1*) was substantially larger than that of their single mutants. Third, both *TaGW2-B1* and *-D1* modulate cell number and length in the outer pericarp of developing grains, with *TaGW2-B1* being more potent. Finally, *TaGW2* homoeologs also affect grain protein content as this parameter was generally increased in the mutants, especially in the lines lacking two or three homoeologs. Consistent with this finding, two wheat end-use quality-related parameters, flour protein content and gluten strength, were considerably elevated in the mutants. Collectively, our data shed light on functional difference between and additive interaction of *TaGW2* homoeologs in the genetic control of grain weight and protein content traits in common wheat, which may accelerate further research on this important gene and its application in wheat improvement.**

Keywords: gene editing mutant, genetic interaction, grain length, grain protein content, grain width, grain weight, homoeolog, pericarp, *Triticum aestivum*.

INTRODUCTION

Plant seeds constitute the most important food source for humans. Consequently, substantial efforts have been devoted to studying the molecular basis underlying the formation and variation of grain traits (Zuo and Li, 2014; Li and Li, 2016). One major goal of this endeavor is to identify the genes controlling grain weight (GW) and its component traits grain width (GWH) and grain length (GL) in order to effectively enhance grain productivity through genetic manipulation (Zuo and Li, 2014; Li and Yang, 2017; Nadolska-Orczyk *et al.*, 2017).

Among the genes that have so far been found to regulate GW, many are involved in controlled degradation of protein through the ubiquitin–proteasome pathway (Li and Li, 2016). One of these genes, *GW2*, has attracted wide attention. This gene, encoding a RING-type E3 ubiquitin ligase, was originally found to regulate rice GW by increasing the cell number of spikelet hulls (Song *et al.*, 2007). There is now increasing evidence that *GW2* homologs exist in other cereal crops (e.g. maize, wheat and sorghum) and may also be involved in control of GW (Li *et al.*, 2010a; Su *et al.*, 2011; Tao *et al.*, 2017). In hexaploid common wheat (*Triticum aestivum* L., AABBDD), three *TaGW2* homoeologs (*TaGW2-A1*, *-B1* and *-D1*) have been identified (Qin *et al.*, 2014), but only *TaGW2-A1* has been proved to affect GW, GWH and GL through mutant analysis (Simmonds *et al.*, 2016). Haplotype and genetic

diversity analyses have also implicated the involvement of *TaGW2-B1* and *-D1* in control of GW (Qin *et al.*, 2014, 2017), but this has yet to be confirmed through mutant analysis. Although the loss-of-function alleles of *TaGW2-A1* have generally been shown to be associated with GW enhancement (Su *et al.*, 2011; Yang *et al.*, 2012; Zhang *et al.*, 2013; Jaiswal *et al.*, 2015; Simmonds *et al.*, 2016), simultaneous silencing of all three *TaGW2* homoeologs via RNA interference (RNAi) has yielded conflicting results, decreasing GW in one report (Bednarek *et al.*, 2012) but increasing GW in another (Hong *et al.*, 2014). Furthermore, potential functional interaction of *TaGW2* homoeologs in wheat grain trait formation has not been studied. The cell biological basis underlying the regulation of GW by *TaGW2* is still obscure. These knowledge gaps are not conducive to a more complete understanding of the function of *TaGW2* and the use of this gene for improving grain traits.

Based on the information presented above, the main objectives of this work were to investigate the function of *TaGW2-B1* and *-D1* and potential functional interaction of *TaGW2* homoeologs in regulating common wheat grain traits. Central to our work was the analysis of four knockout mutants of *TaGW2* developed using clustered regularly interspaced short palindromic repeats (CRISPR)/Cas9-mediated gene editing; these lacked one (*B1* or *D1*), two (*B1* and *D1*) or all three (*A1*, *B1* and *D1*) homoeologs of *TaGW2*. The resultant data provided genetic evidence for the function of *TaGW2-B1* and *-D1* in the control of thousand-grain weight (TGW), a director indicator of GW, as well as that of grain protein content (GPC), a crucial determinant of wheat end-use quality (Shewry, 2007). Furthermore, additive genetic interaction was detected in the action of *TaGW2-B1* and *-D1*, and modulation of maternal pericarp cell growth by the two homoeologs was uncovered. Lastly, the increase in GPC in the mutants was accompanied by considerable elevation in two important quality parameters related to end-use: flour protein content (FPC) and gluten strength. The insights obtained may have important and practical implications for further basic and applied studies of *TaGW2*.

RESULTS

Development of homozygous and transgene-free mutants

We identified three *TaGW2* homoeologs (designated as *TaGW2^{KN}-A1*, *-B1* and *-D1*) in the winter wheat cultivar Kenong 199 (Table S1 in the online Supporting Information), and found that *TaGW2^{KN}-A1* was highly similar to a previously characterized elite allele with a frame-shifting T nucleotide insertion in the coding region (Yang *et al.*, 2012). *TaGW2^{KN}-B1* and *-D1* all carried an intact open reading frame (ORF) (Table S1). The three homoeologs were more than 98% identical in the coding sequence, and exhibited a similar expression profile before and after anthesis, namely being substantially downregulated at 10 and 20 days after anthesis (DAA) but upregulated at 30 DAA (Figure S1). However, at all four stages, the transcript level of *TaGW2^{KN}-B1* was highest, followed by *TaGW2^{KN}-D1* and *TaGW2^{KN}-A1* (Figure S1). A previous study also showed that the expression level of *TaGW2* homoeologs in developing wheat grains could be ranked as *TaGW2-B1* > *TaGW2-D1* > *TaGW2-A1* (Hong *et al.*, 2014).

A single-guide RNA (sgRNA) that matched perfectly with *TaGW2^{KN}-B1* and *TaGW2^{KN}-D1* but had one mismatch with *TaGW2^{KN}-A1* was designed (Figure 1). Using this sgRNA and a transgene-free protocol of CRISPR/Cas9-mediated genome editing (Zhang *et al.*, 2016), 43 independent T_0 mutants were obtained. Because *TaGW2^{KN}-A1* was already a knockout allele (see above), we focused on analyzing *TaGW2^{KN}-B1* and *-D1*. Hence, homozygous lines (*gw2^{kn}-b1*, *gw2^{kn}-d1* and *gw2^{kn}-b1d1*; Figure 1) with frame-shift mutations in *B1*, *D1* or both homoeologs were identified and examined in subsequent investigations. In *gw2^{kn}-b1*, *TaGW2^{KN}-B1* was mutated by the insertion of a frame-shifting adenine nucleotide; in *gw2^{kn}-d1*, *TaGW2^{KN}-D1* was disrupted by the deletion of seven nucleotides; in *gw2^{kn}-b1d1*, *TaGW2^{KN}-B1* and *-D1* carried a single T nucleotide

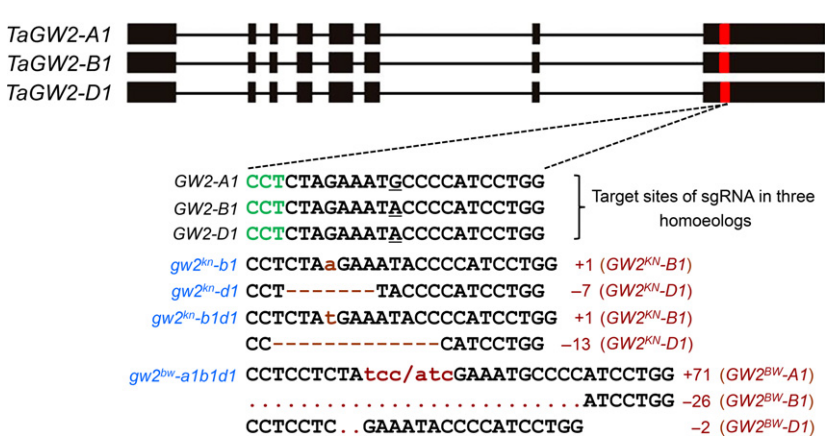

Figure 1. Development of *TaGW2* mutants by CRISPR/Cas9-mediated genome editing.
The exon (vertical bar) and intron (horizontal line) structure of *TaGW2* homoeologs, target sites of single guide RNA (sgRNA) in the homoeologs, and CRISPR/Cas9-induced indels in specific *TaGW2* homoeologs (in brackets) in the four homozygous mutants (*gw2^{kn}-b1*, *gw2^{kn}-d1*, *gw2^{kn}-b1d1* and *gw2^{bw}-a1b1d1*) are depicted. The protospacer-adjacent motif is highlighted in green, and the single nucleotide polymorphism among the three target sites is underlined.

insertion and a 13-bp deletion, respectively, both of which debilitated the reading frame (Figure 1).

Similarly, three *TaGW2* homoeologs (designated as *TaGW2^{BW}-A1*, *-B1* and *-D1*) with an intact ORF were isolated from the spring wheat cultivar Bobwhite (Table S1). *TaGW2^{BW}-A1*, *-B1* and *-D1* greatly resembled their counterparts *TaGW2^{KN}-A1*, *-B1* and *-D1* in their nucleotide sequence (more than 98.3% identical; Table S2). Thus, we edited *TaGW2^{BW}-A1*, *-B1* and *-D1* using the same CRISPR/Cas9 protocol and sgRNA described above, and a homozygous triple mutant (*gw2^{bw}-a1b1d1*), with frame-shifting mutations engineered in all three homoeologs, was developed (Figure 1). The plants of *gw2^{bw}-a1b1d1*, as well as those of *gw2^{kn}-b1*, *gw2^{kn}-d1* and *gw2^{kn}-b1d1*, were all confirmed to be transgene-free by genomic PCR with five primer sets recognizing different parts of the CRISPR/Cas9 construct. Together, four homozygous and transgene-free CRISPR mutants with defined mutation sites in one, two or all three *TaGW2* homoeologs were developed in two varietal backgrounds.

TaGW2 mutants differ in the improvement of grain weight and yield-related traits

The grain samples harvested from Kenong 199, *gw2^{kn}-b1*, *gw2^{kn}-d1* and *gw2^{kn}-b1d1* cultivated in three different environments were assessed. From Table 1, it is clear that the TGW values of the three mutants were all significantly elevated relative to that of the wild-type (WT) control (Kenong 199), with the increases displayed by *gw2^{kn}-b1* and *gw2^{kn}-b1d1* being larger than that of *gw2^{kn}-d1*. Consistent with this result, the GWH and GL values of the mutants were generally and significantly higher than those of the WT control, although the improvement exhibited by *gw2^{kn}-d1* was comparatively smaller (Table 1, Figure 2a). Surprisingly, we noticed that the grains of *gw2^{kn}-b1d1* were morphologically wrinkled compared with those of the WT control, *gw2^{kn}-b1* and *gw2^{kn}-d1* (Figure 2a). Considering all three environments, the increase in TGW was highest in *gw2^{kn}-b1d1* (10.40–13.14%), intermediate in *gw2^{kn}-b1* (5.73–12.04%) and relatively low in *gw2^{kn}-d1* (1.18–8.74%); this order was also found for the increases in GWH and GL displayed by the three mutants (Table 1).

A similar assessment was conducted for Bobwhite and *gw2^{bw}-a1b1d1* with the grains harvested from two different environments. The TGW and GWH of *gw2^{bw}-a1b1d1* were both consistently and significantly larger than those of the WT control (Bobwhite); the GL measurement of *gw2^{bw}-a1b1d1* was also considerably higher than that of the WT control (Figure 2b, Table S3). Like the grains of *gw2^{kn}-b1d1* (Figure 2a), those of *gw2^{bw}-a1b1d1* were also wrinkled (Figure 2b).

Further to the assessment above, grain yield per plant (GYP) was evaluated for the two sets of wheat materials. For Kenong 199 and derivative mutants, the mean GYP

Table 1 Comparison of thousand grain weight (TGW), grain width (GWH) and grain length (GL) between Kenong 199 and three *TaGW2* gene editing mutants.[a]

Environment	Line	TGW (g)	GWH (mm)	GL (mm)
2016-Beijing	Kenong 199	44.52 ± 1.51	3.40 ± 0.07	5.45 ± 0.09
	gw2^{kn}-b1	49.88 ± 1.13** [12.04%]	3.55 ± 0.05** [4.41%]	5.69 ± 0.11* [4.40%]
	gw2^{kn}-d1	45.87 ± 1.12* [3.03%]	3.45 ± 0.07 [1.47%]	5.46 ± 0.08 [0.18%]
	gw2^{kn}-b1d1	50.37 ± 1.06** [13.14%]	3.63 ± 0.07** [6.76%]	5.76 ± 0.06** [5.69%]
2017-Beijing	Kenong 199	44.60 ± 1.83	3.47 ± 0.08	5.24 ± 0.08
	gw2^{kn}-b1	48.73 ± 1.93** [9.26%]	3.56 ± 0.09* [2.59%]	5.57 ± 0.12** [6.30%]
	gw2^{kn}-d1	48.50 ± 1.15** [8.74%]	3.54 ± 0.04* [2.02%]	5.40 ± 0.04** [3.05%]
	gw2^{kn}-b1d1	50.19 ± 0.70** [12.53%]	3.70 ± 0.08** [6.63%]	5.54 ± 0.07** [5.73%]
2017-Gaocheng	Kenong 199	41.36 ± 0.80	3.31 ± 0.05	5.76 ± 0.06
	gw2^{kn}-b1	43.73 ± 0.97** [5.73%]	3.41 ± 0.05** [3.02%]	5.96 ± 0.12** [3.47%]
	gw2^{kn}-d1	41.85 ± 1.31 [1.18%]	3.35 ± 0.07 [1.21%]	5.83 ± 0.08 [1.22%]
	gw2^{kn}-b1d1	45.66 ± 0.86** [10.40%]	3.48 ± 0.06** [5.14%]	6.00 ± 0.08** [4.17%]

[a]The values are presented as mean ± SD. For each line in each environment, the grains from at least 20 plants were combined, with three separate samples taken from the combined seed lot for trait assessment. The percentages in the square brackets indicate the increases over Kenong 199. Statistical comparison was conducted using the independent samples *t*-test in the SPSS program. *$P < 0.05$; **$P < 0.01$.

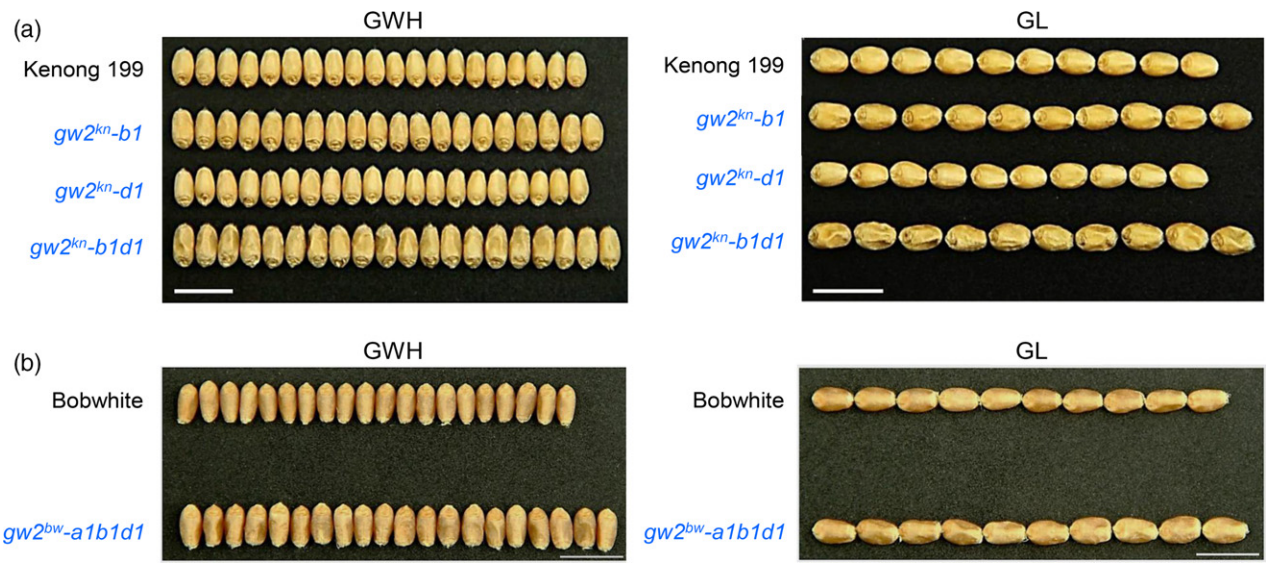

Figure 2. Comparison of grain size and appearance between the wild type and mutant lines.
The comparison was made between the wild type Kenong 199 and derivative mutants (*gw2*^{kn}*-b1*, *gw2*^{kn}*-d1* and *gw2*^{kn}*-b1d1*) (a) or between the wild type Bobwhite and *gw2*^{bw}*-a1b1d1* (b). The grains were aligned to illustrate grain width (GWH) and grain length (GL) between wild-type and mutant lines. Note that the grains of *gw2*^{kn}*-b1d1* and *gw2*^{bw}*-a1b1d1* were morphologically wrinkled. The data shown are representative of three (a) or two (b) environments. Scale bars = 10 mm.

values of *gw2*^{kn}*-b1* and *gw2*^{kn}*-b1d1* were generally higher than that of Kenong 199, with the upper bounds being 10.46 and 16.53%, respectively, but the average GYP of *gw2*^{kn}*-d1* was considerably lower (by 4.14–12.18%) than that of Kenong 199 (Figure S2a). In the case of Bobwhite and its associated mutant, the mean GYP of *gw2*^{bw}*-a1b1d1* was generally higher (up to 14.17% higher) than that of Bobwhite (Figure S2b).

Collectively, the above results indicate substantial improvement of GW and yield-related traits in three *TaGW2* mutants (*gw2*^{kn}*-b1*, *gw2*^{kn}*-b1d1* and *gw2*^{bw}*-a1b1d1*) relative to their WT controls. But *gw2*^{kn}*-d1* shows a comparatively lower improvement of grain-related traits, and exhibits decreased GYP compared with the WT control.

TaGW2 mutants display differential enhancement of grain protein content, flour protein content and gluten strength

By analyzing the data from a previous transcriptome study (Pearce *et al.*, 2015), we found that *TaGW2* homoeologs were expressed in both the pericarp and endosperm tissues in developing wheat grains (Figure S3). This led us to investigate GPC and the contents of seed storage proteins (SSPs) in the mutants and their respective progenitors (Kenong 199 or Bobwhite). Analysis of the grain samples harvested from two different environments (2016-BJ and 2017-BJ) revealed that GPC was considerably elevated in the mutants relative to that of Kenong 199, particularly in *gw2*^{kn}*-b1* (elevated by up to 18.83%) and *gw2*^{kn}*-b1d1* (increased by up to 15.45%) (Table 2). Consistent with this finding, glutenins and gliadins, two major groups of wheat SSPs (Shewry *et al.*, 2003), were generally increased in the three mutants, with *gw2*^{kn}*-b1* and *gw2*^{kn}*-b1d1* showing much larger rises than *gw2*^{kn}*-d1* (Table 2). Similarly, the GPC of *gw2*^{bw}*-a1b1d1* also tended to be higher than that of Bobwhite in two separate environments (Table S3).

Because GPC and the contents of glutenins and gliadins are vital in determining wheat end-use quality (Shewry, 2007), we tested if *gw2*^{kn}*-d1*, *gw2*^{kn}*-b1* and *gw2*^{kn}*-b1d1* might have altered FPC and gluten strength, which are important parameters of wheat end-use quality (Wrigley *et al.*, 2009). In both 2016-BJ and 2017-BJ, the FPC values of *gw2*^{kn}*-d1*, *gw2*^{kn}*-b1* and *gw2*^{kn}*-b1d1* were generally and significantly higher than that of Kenong 199, with the highest percentage increase (up to 24.97%) observed for *gw2*^{kn}*-b1d1* (Figure 3a). The sodium dodecyl sulfate sedimentation volume (SDS-SV), signifying gluten strength (Ross and Bettge, 2009), was also significantly higher in the three mutants than in Kenong 199, with *gw2*^{kn}*-b1d1* again showing the highest percentage increase (up to 18.53%) (Figure 3b).

Clearly, the three parameters related to end-use quality, i.e. GPC, FPC and SDS-SV, are all enhanced in the examined *TaGW2* mutants, especially for *gw2*^{kn}*-b1*, *gw2*^{kn}*-b1d1* and *gw2*^{bw}*-a1b1d1*. The enhancement is associated with increased levels of accumulation of glutenins and gliadins.

TaGW2 mutants exhibit altered growth of maternal pericarp cells

In rice, knockout of *GW2* enhances GW and GWH by promoting the number of spikelet hull cells and the size of endosperm cells (Song *et al.*, 2007). Therefore we analyzed cell growth in the developing grains of Kenong 199 and

Table 2 Comparison of grain protein content (GPC) and the glutenin and gliadin contents between Kenong 199 and three *TaGW2* gene editing mutants.[a]

Environment	Line	GPC (%)	Total glutenin (μg/mg grain)	Total gliadin (μg/mg grain)
2016-Beijing	Kenong 199	12.43 ± 0.19	30.29 ± 0.41	47.11 ± 0.91
	gw2^{kn}-b1	14.77 ± 0.35** [18.83%]	35.50 ± 10.51** [17.20%]	54.74 ± 16.13** [16.20%]
	gw2^{kn}-d1	12.81 ± 0.18 [3.01%]	30.30 ± 1.28 [0.03%]	47.19 ± 0.63 [0.17%]
	gw2^{kn}-b1d1	14.35 ± 0.05** [15.45%]	31.28 ± 0.17* [3.27%]	56.39 ± 1.00** [19.70%]
2017-Beijing	Kenong 199	13.28 ± 0.15	30.83 ± 0.23	60.02 ± 0.32
	gw2^{kn}-b1	14.21 ± 0.66* [7.00%]	32.22 ± 1.89* [4.51%]	63.77 ± 1.88* [6.25%]
	gw2^{kn}-d1	14.69 ± 0.70* [10.84%]	31.89 ± 0.26* [3.44%]	68.34 ± 0.34** [13.86%]
	gw2^{kn}-b1d1	14.85 ± 0.41** [11.82%]	33.41 ± 0.32** [8.37%]	70.90 ± 1.23** [18.13%]

[a]The values are presented as mean ± SD. For each line in each environment, the grains from at least 20 plants were combined, with three separate samples taken from the combined seed lot for trait assessment. The percentages in the square brackets indicate the increases over Kenong 199. Statistical comparison was conducted using the independent samples *t*-test in the SPSS program. *$P < 0.05$; **$P < 0.01$.

derivative mutants. The grains at 21 DAA were employed in this analysis because they reached maximum fresh weight around this stage. The cells in the outer pericarp were mainly examined because the three *TaGW2* homoeologs were highly expressed there (Figure S3). To simplify the task, the middle portion along the longitudinal axis of the grains was used for the analysis (Figure 4a). In the median sections (Figure 4b), the total number of cells in the surface layer of the outer pericarp was significantly higher in *gw2^{kn}-b1* and *gw2^{kn}-b1d1* than that in Kenong 199, with *gw2^{kn}-b1d1* showing a much bigger increase; *gw2^{kn}-d1* also exhibited some increase in this parameter although this was not significant (Figure 4c). Cryo-scanning electron microscopy revealed that the surface pericarp cells of the three mutants were much longer than those of Kenong 199 (Figure 4d). Upon closer examination, substantial differences were found among Kenong 199 and mutant lines in the two lateral sides of the outer pericarp (indicated in Figure 4a). In Kenong 199, the outer pericarp contained mostly two layers of cells (Figure 4e), whereas in *gw2^{kn}-b1* and *gw2^{kn}-d1* four cell layers were commonly observed in the outer pericarp (Figure 4f, g). For *gw2^{kn}-b1d1*, the outer pericarp was generally composed of three cell layers (Figure 4 h).

Together, these results show that the growth of maternal pericarp cells in *gw2^{kn}-b1*, *gw2^{kn}-d1* and *gw2^{kn}-b1d1* is altered in multiple ways and that the alteration differs among the three mutants.

DISCUSSION

TaGW2 homoeologs experienced substantial selection in polyploidization, domestication and artificial breeding of common wheat (Qin *et al.*, 2014, 2017), indicating that they may have played pivotal roles in the increase in GW that occurred during the evolution of modern wheat cultivars from primitive ancestral species. However, prior to this work there was only limited information on the involvement of *TaGW2-B1* and *-D1* in regulation of GW. The presence of three homoeologs with high sequence similarities may have hampered the functional analysis of *TaGW2*. To overcome this difficulty, we analyzed a unique series of gene editing mutants that had knockout mutations in one, two or all three *TaGW2* homoeologs. The results obtained have allowed us to more completely explore the functions of *TaGW2* homoeologs in the genetic control of common wheat grain traits and the relevant mechanisms.

Insights into the functions of *TaGW2* homoeologs

First, both *TaGW2-B1* and *-D1* function in the genetic control of GW, and they participate in the negative regulation of this trait. This insight is supported by the finding that knocking out *TaGW2^{KN}-B1*, *TaGW2^{KN}-D1* or both promoted significant increases of TGW and its component trait GWH and GL (Table 1). Moreover, the effect conferred by *TaGW2-B1* is stronger than that by *TaGW2-D1* because *gw2^{kn}-b1* consistently exhibited higher increases of TGW, GWH and GL than *gw2^{kn}-d1* (Table 1). Second, there may exist an additive interaction between *TaGW2-B1* and *-D1* as the increases of TGW, GWH and GL shown by *gw2^{kn}-b1d1* were generally larger than those of *gw2^{kn}-b1* or *gw2^{kn}-d1* alone (Table 1). Third, both *TaGW2-B1* and *-D1* modulate cell number and length in the outer pericarp of developing grains, with the potency of *TaGW2-B1* being greater (Figure 4). Lastly, *TaGW2* homoeologs also take part in the genetic control of GPC, as this parameter was generally increased in the mutants, especially in the lines lacking

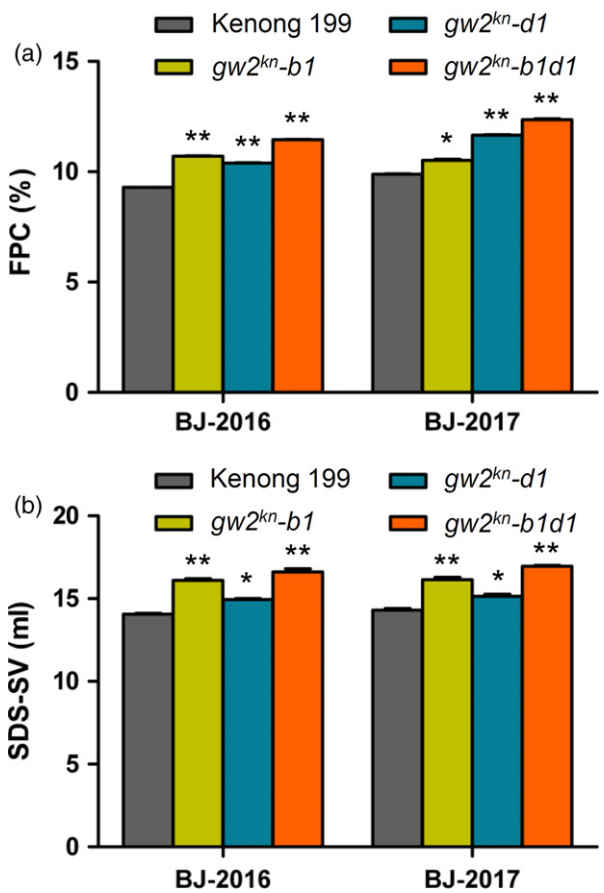

Figure 3. Evaluation of flour protein content (FPC) and sodium dodecyl sulfate sedimentation volume (SDS-SV) in Kenong 199 and derivative *TaGW2* mutants.

Flour protein content (% of flour) (a) and SDS-SV (ml) (b) were determined for Kenong 199 and three *TaGW2* mutants ($gw2^{kn}$-*b1*, $gw2^{kn}$-*d1* and $gw2^{kn}$-*b1d1*) using the grain samples harvested from two environments (BJ-2016 and BJ-2017). The means (±SD) of the three mutants were each compared with that of Kenong 199 using the independent samples *t*-test. $*P < 0.05$; $**P < 0.01$.

two or three homoeologs (Tables 2 and S3). Like their functional difference in the TGW trait, *TaGW2-B1* is again more powerful than *TaGW2-D1* in affecting GPC and the glutenin and gliadin content in common wheat grains (Table 2).

In line with their increases in TGW (Tables 1 and S3), the GYP values of $gw2^{kn}$-*b1*, $gw2^{kn}$-*b1d1* and $gw2^{bw}$-*a1b1d1* were higher than those of their WT controls (Kenong 199 or Bobwhite; Figure S2), indicating that increase in TGW contributes to elevation of GYP in the mutants. Consistent with the rises in GPC (Table 2), $gw2^{kn}$-*b1* $gw2^{kn}$-*d1* and $gw2^{kn}$-*b1d1* displayed elevated FPC and gluten strength (Figure 3), suggesting improved end-use quality in the three mutants. Because $gw2^{kn}$-*b1d1* consistently exhibited higher GYP, FPC and SDS-SV values than $gw2^{kn}$-*b1* (Figures S2a and 3), it is possible that additive interaction may also operate in the influence on wheat yield and end-use quality traits by *TaGW2-B1* and *-D1*. However, more systematic and rigorous studies are needed to ascertain the dissimilar effects of *TaGW2* homoeologs on wheat yield and end-use quality, considering that these traits are complex and controlled by multiple genes.

Understanding homoeolog differences and interactions is indispensable for objectively resolving the function of common wheat genes (Borrill *et al.*, 2015). In this regard, the insights outlined above represent an advance towards understanding the functions of *TaGW2* homoeologs. In agreement with our finding on the functional superiority of *TaGW2-B1* over *TaGW2-D1*, a previous haplotype analysis showed that *TaGW2-B1* could explain a higher percentage of variation in TGW than *TaGW2-A1* in common wheat cultivars (Qin *et al.*, 2014). Thus, *TaGW2-B1* may be functionally superior to both *TaGW2-A1* and *-D1*. The reason behind the functional superiority of *TaGW2-B1* is unknown at present, but it is interesting to note that both our work (Figure S1) and that of Hong *et al.* (2014) showed that *TaGW2-B1* was more highly expressed than *TaGW2-A1* and *-D1* in the developing grains. We note that in Figure S3 the expression level of *TaGW2-B1* was no higher than that of *TaGW2-D1*, but the dataset used for generating this figure was obtained by analyzing a different cultivar and using dissected grain parts (Pearce *et al.*, 2015). Nevertheless, the expression level of *TaGW2-B1* was much higher than that of *TaGW2-A1* in Figure S3. Bednarek *et al.* (2012) demonstrated that TaGW2 homoeologs possess E3 ligase activity and shuttle between the cytoplasmic and nuclear compartments. It is possible that TaGW2-B1 may play a more dominant role than TaGW2-A1 and -D1 in the controlled degradation of certain key cellular proteins through the proteasome pathway during grain development. However, further research is needed to verify this possibility.

Modulation of cell growth in maternal tissues has been considered as a basic step in the regulation of GW, GWH and GL by a number of genes in Arabidopsis and rice (Zuo and Li, 2014; Li and Li, 2016). A recent study showed that a major quantitative trait locus on wheat chromosome 5A promoted GW by enhancing both GL and GWH, with a substantial increase in cell length found in the pericarp (Brinton *et al.*, 2017). Based on the changes in carpel/grain size in developing wheat grains, Simmonds *et al.* (2016) indicated that *TaGW2-A1* may regulate GW by acting on the maternal tissue. Here, by coupling genetic and cell biological investigations, we observed that knocking out *TaGW2-B1*, *-D1* or both resulted in different degrees of enhancement in pericarp cell number and length (Figure 4). Consequently, we suggest that *TaGW2* homoeologs modulate maternal pericarp cell growth, thereby affecting GWH, GL and TGW. However, the cell number and length increases observed for $gw2^{kn}$-*b1d1* were not simply a sum of the effects by $gw2^{kn}$-*b1* or $gw2^{kn}$-*d1* alone, indicating

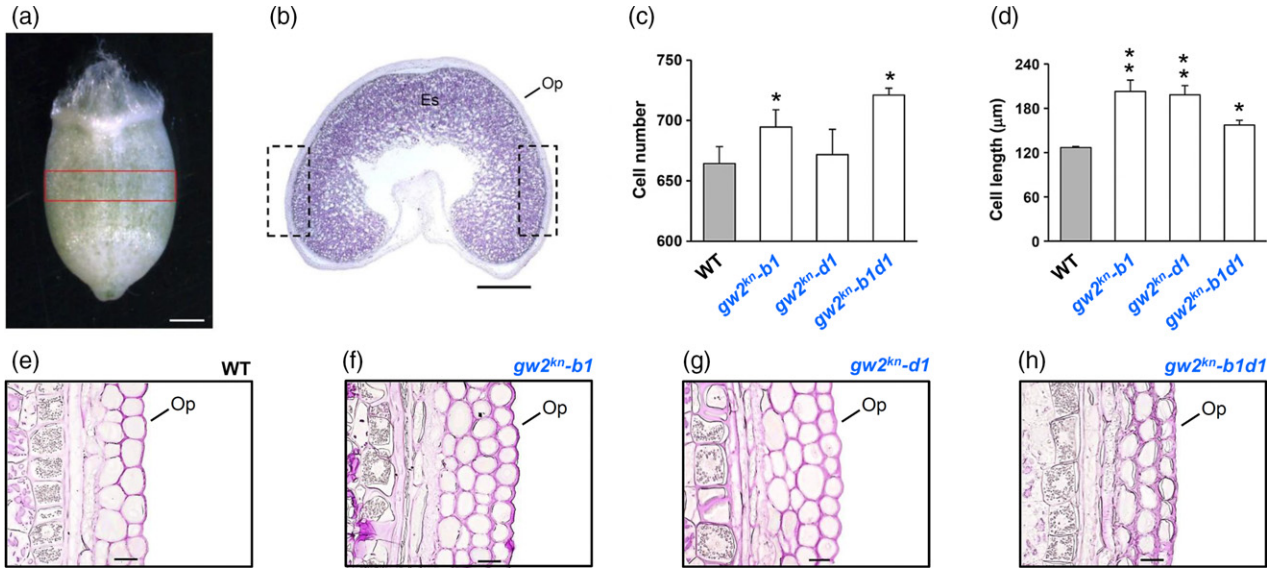

Figure 4. Effects of knocking out *TaGW2-B1*, *-D1* or both on the pericarp cell growth of developing grains.
(a) A typical developing grain of Kenong 199 at 21 days after anthesis (DAA). The middle portion used for light and cryo-scanning electron microscopy experiments in this work is boxed in red. Scale bar = 1 mm. (b) A median section cut from the middle portion of a developing grain of Kenong 199 at 21 DAA. The boxed lateral sides were examined in detail in (e)–(h). ES, endosperm; Op, outer pericarp. Scale bar = 1 mm. (c), (d) Comparison of cell number and length between Kenong 199 (wild-type control, WT) and three mutant lines. For each genotype, the median sections cut from 10 different grains were examined for the number of cells in the surface layer of the outer pericarp; the middle portions of 20 different grains were examined by scanning electron microscopy to reveal the length of the cells in the surface layer of the outer pericarp. The means (±SD) of the mutants were each compared with that of the WT control using the independent samples *t*-test. $*P < 0.05$; $**P < 0.01$. (e)–(h) Cell layers in the lateral sides of the outer pericarp (OP) in Kenong 199 (WT control) and three mutant lines. The lateral sides examined are indicated in (b). Each image was representative of 10 different grains. Scale bar = 100 μm.

complex functional interactions between *TaGW2* homoeologs in modulating the growth of pericarp cells.

The genetic basis of GPC has been investigated in many studies in wheat (Shewry, 2007; Nigro *et al.*, 2014; Würschum *et al.*, 2016). At the molecular level, three important genes regulating wheat GPC, namely *Gpc-B1*, *SPA* and *DEMETER*, have been characterized (Uauy *et al.*, 2006; Ravel *et al.*, 2009; Wen *et al.*, 2012). The latter two genes regulate GPC by controlling the expression of glutenin and gliadin genes. This coincides with our observation that increases in GPC in the single and double mutants of *TaGW2* were associated with upregulated accumulation of glutenins and gliadins (Table 2). Considering the E3 ligase activity of TaGW2 protein and their likely involvement in the proteasome pathway (Bednarek *et al.*, 2012), it will be interesting to test if the effects of *TaGW2* homoeologs on GPC may be brought about by regulating the turnover of certain key proteins (e.g. *SPA* and *DEMETER*) controlling the expression of glutenin and gliadin genes in wheat grains.

A further finding made in this work is that the grains of $gw2^{kn}$*-b1d1* and $gw2^{bw}$*-a1b1d1*, but not those of $gw2^{kn}$*-b1* and $gw2^{kn}$*-d1*, were wrinkled (Figure 2). Because $TaGW2^{KN}$*-A1* is already a naturally evolved loss-of-function allele (see above), $gw2^{kn}$*-b1d1* was actually a triple mutant and $gw2^{kn}$*-b1* and $gw2^{kn}$*-d1* were both double mutants. Thus, grain wrinkling is a problem shared by two triple mutants in two varietal (Kenong 199 and Bobwhite) backgrounds, but it does not occur in the double mutants lacking *TaGW2-A1* and *-B1* or *TaGW2-A1* and *-D1*. This leads us to speculate that grain wrinkling in the triple mutants may be caused by excessive reduction of *TaGW2* function. We did not find any significant difference in seed starch content between Kenong 199 and $gw2^{kn}$*-b1d1* cultivated in two environments (Table S4). Therefore the grain wrinkling phenotype displayed by $gw2^{kn}$*-b1d1* is unlikely to be caused by alteration in seed starch content. Further studies involving transcriptomic and proteomic experiments may yield useful clues to understanding the observed grain wrinkling phenotype.

Finally, our findings that both $gw2^{kn}$*-b1d1* and $gw2^{bw}$*-a1b1d1* exhibited increases in TGW in multiple environments (Tables 1 and S3) contrast with the report that simultaneously silencing three *TaGW2* homoeologs by RNAi decreased TGW (Bednarek *et al.*, 2012). Our results, together with the data reported by Hong *et al.* (2014), argue strongly that reducing the function of all three *TaGW2* copies will most probably increase, rather than decrease, GW, although this increase was accompanied by a grain wrinkling problem.

Implications for further research

From the points discussed above, several new areas central to understanding the individual and combined actions

of *TaGW2* homoeologs in regulating TGW and GPC and the cell biological and underlying biochemical basis are now open for future research. In addition, our data may have practical implications for the use of *TaGW2* in wheat breeding.

First, knockout mutants of *TaGW2-B1* or combinations with those of *TaGW2-A1* may now be used to enhance TGW and GPC in common wheat. As discussed above, the enhancement effects conferred by *TaGW2-B1* mutants are probably much better than those conferred by the *TaGW2-A1* alleles characterized so far. *TaGW2-B1* mutants may be identified in wheat germplasm; alternatively, as exemplified in this work, they can also be created in the desired genetic backgrounds using efficient transgene-free gene editing methods (Zhang *et al.*, 2016). Second, the substantial increases in TGW and GPC augmented by knocking out all three *TaGW2* homoeologs may be harnessed to improve the yield and quality traits of wheat, providing that the grain wrinkling problem can be overcome satisfactorily. A possible solution to the problem is to find genetic suppressor(s) of the grain wrinkling phenotype, and we are now in the process of investigating this possibility.

In summary, our work sheds light on functional difference and additive interaction of *TaGW2-B1* and *-D1* in the genetic control of GW and protein content traits in common wheat, which may stimulate further research on this important gene and its application in wheat improvement.

EXPERIMENTAL PROCEDURES

Cloning and sequence analysis of *TaGW2* homoeologs

The cDNA coding region of *TaGW2-A1*, *-B1* and *-D1* homoeologs was isolated from Kenong 199 and Bobwhite using RT-PCR as described previously (Yang *et al.*, 2012; Hong *et al.*, 2014). The forward and reverse primers used were GW2-CDS-F (5′-ATGGG GAACAGAATAGGAGGGAGG-3′) and GW2-CDS-R (5′-TTACAAC CATGCCAACCCTTGCGT-3′), respectively. The cDNA and deduced amino acid sequences for the six genes are listed in Table S1. Sequence comparisons were conducted using Clustal Omega (http://www.ebi.ac.uk/Tools/msa/clustalo/).

Investigation of the expression of *TaGW2* homoeologs

The expression profiles of $TaGW2^{KN}$*-A1*, *-B1* and *-D1* in the developing grains of Kenong 199 were investigated using a HiSeq transcriptomic data set, generated by sequencing the total RNA samples extracted from unfertilized caryopses and the grains at 10, 20 and 30 DAA. For each time point, three biological replicates were sequenced. Detailed analysis of the RNA sequencing experiment will be reported elsewhere. The software Bowtie (Ben *et al.*, 2009) was used to align HiSeq reads to the coding sequence of $TaGW2^{KN}$*-A1*, *-B1* and *-D1*, respectively, with the wrongly mapped reads corrected by manual inspection. The expression level was presented as reads per kilobase per million mapped reads (Figure S1).

The expression patterns of *TaGW2* homoeologs in the endosperm, inner pericarp and outer pericarp tissues were investigated with the transcriptomic data deposited in the WheatEXP website (https://wheat.pw.usda.gov/WheatExp/). Briefly, the cDNA coding sequence of $TaGW2^{KN}$*-A1*, *-B1* and *-D1* was blasted in WheatEXP. This identified the three *TaGW2* homoeologs (*Traes_6AS_3F739-BAFF.2*, *Traes_6BS_28B1B89B5.2* and *Traes_6DS_9452342E3.2*) annotated by the International Wheat Genome Sequencing Consortium. The expression patterns of the homoeologs in three layers of developing wheat grains (i.e. outer pericarp, inner pericarp and endosperm, collected at 12 DAA; Figure S2) were then obtained using the transcriptomic data reported by Pearce *et al.* (2015).

Development and growth of mutants

The 43 T_0 gene editing mutants of *TaGW2* developed using the immature embryos of Kenong 199 were described in our previous publication (Zhang *et al.*, 2016). In brief, these mutants were prepared through transient expression of CRISPR/Cas9 DNA (TECCDNA) or RNA in the immature embryos with a sgRNA targeting the eighth exon (Figure 1). The two methods yielded 26 and 17 T_0 mutants, respectively. Homozygous $gw2^{kn}$*-b1*, $gw2^{kn}$*-d1* and $gw2^{kn}$*-b1d1* seedlings were identified in the T_2 population through sequencing amplicons carrying the target sites. The homozygous mutant lines and their WT progenitor were then cultivated in three different environments, i.e. a net house in the field in Beijing in 2016 and controlled field plots in Beijing and Gaocheng (Hebei Province, China), respectively, in 2017. Standard agronomic practices were applied to promote seed setting.

TECCDNA was employed to edit the *TaGW2* homoeologs in Bobwhite as described above. A total of 2000 immature embryos were used in the transformation experiment, which yielded 47 T_0 mutants. Three T_0 mutants with indels in all six *TaGW2* alleles were identified; their T_2 seeds were employed to identify a homozygous mutant (i.e. $gw2^{bw}$*-a1b1d1*) with frame-shifting indels in $TaGW2^{BW}$*-A1*, *-B1* and *-D1*. The $gw2^{bw}$*-a1b1d1* plants were grown in the net house in Beijing as outlined above, with grain samples harvested in 2016 and 2017, respectively. The grains from WT Bobwhite plants were similarly harvested, and served as controls in the experiments.

Neither $gw2^{kn}$*-b1*, $gw2^{kn}$*-d1* and $gw2^{kn}$*-b1d1* seedlings nor those of $gw2^{bw}$*-a1b1d1* were found to contain the integration sites of Cas9 and sgRNA constructs when checked by PCR with the primer sets detailed by Zhang *et al.* (2016).

Phenotypic assessment

For each line in each environment the grains from at least 20 plants were harvested and combined for phenotypic assessment; the mean TGW, GWH and GL values were determined using three separate grain samples with an automatic seed trait analysis system (Model SC-G, Wseen Ltd, http://hzwseen.foodmate.net/). The GYP was assessed by measuring and averaging the GW of seven plants per genotype per environment. The FPC and SDS-SV were measured for the desired genotypes following the method detailed by Li *et al.* (2010b), with three different flour samples used per genotype per environment.

Light microscopy

The following steps were carried out at room temperature i.e. 23°C–25°C unless otherwise stated. The developing grains were collected from Kenong 199 and $gw2^{kn}$*-b1*, $gw2^{kn}$*-d1* and $gw2^{kn}$*-b1d1* plants at 21 DAA. The two ends of the grains were gently removed under FAA fixative (70% alcohol, 5% acetic acid, 0.02% formaldehyde), with the middle portion fixed in FAA for 24 h at 4°C. Afterwards, the fixed materials were gradually dehydrated

using 70, 80, 90, 95 and 100% alcohol solutions (1 h in each solution and with gentle rotation). The resultant samples were sequentially treated with three LR White acrylic resin/alcohol mixtures (1:2, 1:1 and 2:1, 3 h in each mixture), followed by two consecutive infiltrations in 100% LR White (8 h each). The LR White resin used was of medium grade (Sigma-Aldrich, http://www.sigmaaldrich.com/). Subsequently, each of the infiltrated grain materials was embedded in 300 μl of pure LR White, with the polymerization accomplished at 65°C for 24 h. The sections (1.5 μm thick) were cut with a diamond knife on a Leica microtome (Leica Microsystems, https://www.leica-microsystems.com/). They were then treated with the periodic acid-Schiff regent and counter-stained with 0.1% Coomassie Bright Blue, as described previously (Wu *et al.*, 2016). The sections were examined under a Leica DM2500 microscope (Leica Microsystems) and the images taken using a digital camera.

Cryo-scanning electron microscopy and measurement of cell length

At 21 DAA, the developing grains were carefully separated from the surrounding glumes, attached to aluminum stubs and examined following the method reported by Mazurek *et al.* (2013). The cryo-preparation system used was Quorum PP3000T (Quorum Technologies Ltd, https://www.quorumtech.com/), and the scanning electron microscope employed was a Hitachi S-3000N (Hitachi High-Technologies, https://www.hitachi-hightech.com/global/). For each line (Kenong 199, *gw2*^{kn}*-b1*, *gw2*^{kn}*-d1* and *gw2*^{kn}*-b1d1*) at least five different grains were examined, with the images being taken from the middle portion of the grain along the longitudinal axis. The captured images were analyzed using ImageJ software (https://imagej.nih.gov/ij/). The mean length of surface cells in the outer pericarp of each line was calculated by measuring approximately 400 cells.

Determination of GPC and the glutenin and gliadin contents

For each line, GPC was assayed using wholemeal flour prepared with a cyclone hammer mill from 50 g of grains. The assay was accomplished on an Organic Elemental Analysis Flash 2000 elemental analyzer (Thermo Scientific Corporation, https://www.thermofisher.com/) following Method 46-30 recommended by the American Association of Cereal Chemists (AACC International, 2000). Three measurements were performed using separate grain samples. The glutenin and gliadin contents in the grains were measured using reverse phase-high performance liquid chromatography (Marchylo *et al.*, 1989), with three determinations conducted for each line with separate grain samples.

Statistical analysis

Numerical phenotypical data were presented as means ± SD. Statistical analysis of the means was performed by an independent samples *t*-test in the SPSS program (SPSS Inc., https://www.ibm.com/analytics/data-science/predictive-analytics/spss-statistical-software/).

ACKNOWLEDGEMENTS

This research was supported by the National Key R&D Program of China (grants 2016YFD0100500 and 2016YFD0101804) and the National Transgenic Science and Technology Program (2016ZX08010-002). The authors thank Mr Yanbao Tian for assisting with the microscopy experiments.

CONFLICT OF INTEREST

The authors declare no conflict of interest.

SUPPORTING INFORMATION

Additional Supporting Information may be found in the online version of this article.

Figure S1. Expression profiles of *TaGW2*^{KN}*-A1, -B1* and *-D1* in the developing grains of Kenong 199.

Figure S2. Comparison of grain yield per plant between Kenong 199 and *TaGW2* mutant lines.

Figure S3. Expression patterns of *TaGW2-A1, -B1* and *-D1* in the endosperm and pericarp tissues of developing wheat grains.

Table S1. The cDNA and deduced protein sequences of *TaGW2* homoeologs cloned in this study.

Table S2. Nucleotide sequence identities between the *TaGW2* homoeologs of Kenong 199 and Bobwhite.

Table S3. Comparison of thousand-grain weight, grain width, grain length and grain protein content between Bobwhite and the *gw2*^{bw}*-a1b1d1* mutant.

Table S4. Comparison of seed starch content between Kenong 199 and *gw2*^{kn}*-b1d1*.

REFERENCES

AACC International (2000) Method 46-30, Crude protein combustion method. In *of the American Association of Cereal Chemists*, 10th edn. (Methods, Approved, ed). St Paul, Minnesota: AACC International.

Bednarek, J., Boulaflous, A., Girousse, C., Ravel, C., Tassy, C., Barret, P., Bouzidi, M.F. and Mouzeyar, S. (2012) Down-regulation of the *TaGW2* gene by RNA interference results in decreased grain size and weight in wheat. *J. Exp. Bot.* **63**, 5945–5955.

Ben, L., Cole, T., Mihai, P. and Steven, L.S. (2009) Ultrafast and memory-efficient alignment of short DNA sequences to human genome. *Genome Biol.* **10**, R25.

Borrill, P., Adamski, N. and Uauy, C. (2015) Genomics as the key to unlocking the polyploid potential of wheat. *New Phytol.* **208**, 1008–1022.

Brinton, J., Simmonds, J., Minter, F., Leverington-Waite, M., Snape, J. and Uauy, C. (2017) Increased pericarp cell length underlies a major quantitative trait locus for grain weight in hexaploid wheat. *New Phytol.* **215**, 1026–1038.

Hong, Y., Chen, L., Du, L.P., Su, Z., Wang, J., Ye, X., Qi, L. and Zhang, Z. (2014) Transcript suppression of *TaGW2* increased grain width and weight in bread wheat. *Funct. Integr. Genomics*, **14**, 341–349.

Jaiswal, V., Gahlaut, V., Mathur, S. *et al.* (2015) Identification of novel SNP in promoter sequence of *TaGW2-6A* associated with grain weight and other agronomic traits in wheat (*Triticum aestivum* L.). *PLoS ONE*, **10**, e0129400.

Li, N. and Li, Y. (2016) Signaling pathways of seed size control in plants. *Curr. Opin. Plant Biol.* **33**, 23–32.

Li, W. and Yang, B. (2017) Translational genomics of grain size regulation in wheat. *Theor. Appl. Genet.* **130**, 1765–1771.

Li, Q., Li, L., Yang, X., Warburton, M.L., Bai, G., Dai, J., Li, J. and Yan, J. (2010a) Relationship, evolutionary fate and function of two maize co-orthologs of rice *GW2* associated with kernel size and weight. *BMC Plant Biol.* **10**, 143.

Li, Y., Zhou, R., Branlard, G. and Jia, J. (2010b) Development of introgression lines with 18 alleles of glutenin subunits and evaluation of the effects of various alleles on quality related traits in wheat (*Triticum aestivum* L.). *J. Cereal Sci.* **51**, 127–133.

Marchylo, B.A., Kruger, J.E. and Hatcher, D.W. (1989) Quantitative reversed-phase high-performance liquid chromatographic analysis of wheat storage proteins as a potential quality prediction tool. *J. Cereal Sci.* **9**, 113–130.

Mazurek, S., Mucciolo, A., Humbel, B.M. and Nawrath, C. (2013) Transmission Fourier transform infrared microspectroscopy allows simultaneous

assessment of cutin and cell-wall polysaccharides of *Arabidopsis* petals. *Plant J.* **74**, 880–891.

Nadolska-Orczyk, A., Rajchel, I.K., Orczyk, W. and Gasparis, S. (2017) Major genes determining yield-related traits in wheat and barley. *Theor. Appl. Genet.* **130**, 1081–1098.

Nigro, D., Blanco, A., Anderson, O.D. and Gadaleta, A. (2014) Characterization of ferredoxin-dependent glutamine-oxoglutarate amidotransferase (Fd-GOGAT) genes and their relationship with grain protein content QTL in wheat. *PLoS ONE* **9**, e103869.

Pearce, S., Huttly, A.K., Prosser, I.M. *et al.* (2015) Heterologous expression and transcript analysis of gibberellin biosynthetic genes of grasses reveals novel functionality in the GA3ox family. *BMC Plant Biol.* **15**, 130.

Qin, L., Hao, C., Hou, J., Wang, Y., Li, T., Wang, L., Ma, Z. and Zhang, X. (2014) Homologous haplotypes, expression, genetic effects and geographic distribution of the wheat yield gene *TaGW2*. *BMC Plant Biol.* **14**, 107.

Qin, L., Zhao, J., Li, T., Hou, J., Zhang, X. and Hao, C. (2017) *TaGW2*, a good reflection of wheat polyploidization and evolution. *Front. Plant Sci.* **8**, 318.

Ravel, C., Martre, P., Romeuf, I., Dardevet, M., El-Malki, R., Bordes, J., Duchateau, N., Brunel, D., Balfourier, F. and Charmet, G. (2009) Nucleotide polymorphism in the wheat transcriptional activator Spa influences its pattern of expression and has pleiotropic effects on grain protein composition, dough viscoelasticity, and grain hardness. *Plant Physiol.* **151**, 2133–2144.

Ross, A.S. and Bettge, A.D. (2009) Passing the test on wheat end-use quality. In *Wheat Science and Trade* (Carver, B.F., ed). Iowa: Wiley-Blackwell, pp. 455–493.

Shewry, P.R. (2007) Improving the protein content and composition of cereal grain. *J. Cereal Sci.* **46**, 239–250.

Shewry, P.R., Halford, N.G. and Lafiandra, D. (2003) Genetics of wheat gluten proteins. *Adv. Genet.* **49**, 111–184.

Simmonds, J., Scott, P., Brinton, J., Mestre, T.C., Bush, M., Del Blanco, A., Dubcovsky, J. and Uauy, C. (2016) A splice acceptor site mutation in *TaGW2-A1* increases thousand grain weight in tetraploid and hexaploid wheat through wider and longer grains. *Theor. Appl. Genet.* **129**, 1099–1112.

Song, X.J., Huang, W., Shi, M., Zhu, M.Z. and Lin, H.X. (2007) A QTL for rice grain width and weight encodes a previously unknown RING-type E3 ubiquitin ligase. *Nat. Genet.* **39**, 623–630.

Su, Z., Hao, C., Wang, L., Dong, Y. and Zhang, X. (2011) Identification and development of a functional marker of *TaGW2* associated with grain weight in bread wheat (*Triticum aestivum* L.). *Theor. Appl. Genet.* **122**, 211–223.

Tao, Y., Mace, E.S., Tai, S., Cruickshank, A., Campbell, B.C., Zhao, X., Van Oosterom, E.J., Godwin, I.D., Botella, J.R. and Jordan, D.R. (2017) Whole-genome analysis of candidate genes associated with seed size and weight in *sorghum bicolor* reveals signatures of artificial selection and insights into parallel domestication in cereal crops. *Front. Plant Sci.* **8**, 1237.

Uauy, C., Distelfeld, A., Fahima, T., Blechl, A. and Dubcovsky, J. (2006) A NAC gene regulating senescence improves grain protein, Zn, and Fe content in wheat. *Science*, **314**, 1298–1301.

Wen, W., Wen, N., Pang, J. *et al.* (2012) Structural genes of wheat and barley 5-methylcytosine DNA glycosylases and their potential applications for human health. *Proc. Natl Acad. Sci. USA*, **109**, 20543–20548.

Wrigley, C., Asenstorfer, R., Batey, I., Cornish, G., Day, L., Mares, D. and Mrva, K. (2009) The biochemical and molecular basis of wheat quality. In *Wheat Science and Trade* (Carver, B.F., ed). Iowa: Wiley-Blackwell, pp. 495–520.

Wu, X., Liu, J., Li, D. and Liu, C.M. (2016) Rice caryopsis development II: dynamic changes in the endosperm. *J. Integr. Plant Biol.* **58**, 786–798.

Würschum, T., Leiser, W.L., Kazman, E. and Longin, C.F. (2016) Genetic control of protein content and sedimentation volume in European winter wheat cultivars. *Theor. Appl. Genet.* **129**, 1685–1696.

Yang, Z., Bai, Z., Li, X., Wang, P., Wu, Q., Yang, L., Li, L. and Li, X. (2012) SNP identification and allelic-specific PCR markers development for *TaGW2*, a gene linked to wheat kernel weight. *Theor. Appl. Genet.* **125**, 1057–1068.

Zhang, X., Chen, J., Shi, C., Chen, J., Zheng, F. and Tian, J. (2013) Function of *TaGW2-6A* and its effect on grain weight in wheat (*Triticum aestivum* L.). *Euphytica*, **192**, 347–357.

Zhang, Y., Liang, Z., Zong, Y., Wang, Y., Liu, J., Chen, K., Qiu, J.L. and Gao, C. (2016) Efficient and transgene-free genome editing in wheat through transient expression of CRISPR/Cas9 DNA or RNA. *Nat. Commun.* **7**, 12617.

Zuo, J. and Li, J. (2014) Molecular genetic dissection of quantitative trait loci regulating rice grain size. *Annu. Rev. Genet.* **48**, 99–118.